

Architecture for Combined Energy and Attitude Control System

Ibrahim Mustafa Mehedi, Renuganth Varatharajoo, Harlisya Harun and Mohd Nizam Filipski
Department of Aerospace Engineering, University Putra Malaysia
43400 Serdang, Selangor, Malaysia

Abstract: Combining the energy and attitude control system is a feasible technology for small satellites to improve the space missions. In this Combined Energy and Attitude Control System (CEACS) a double rotating flywheel is used to replace the conventional battery for energy storage as well as to control the attitude of an earth oriented satellite. Each flywheel is to be controlled in the torque mode. The energy and attitude inputs for the flywheels' control architecture are also in the torque mode. All related mathematical representation along with the relevant transfer functions and the required numerical calculation are developed. The goals are to analyze the attitude performance with respect to the ideal and non-ideal test cases for a chosen reference mission.

Key words: Attitude Control, Energy Storage, Flywheel

INTRODUCTION

Flywheels are used as a storage element of the power system and also as a satellite attitude control device forming a "Combined Energy and Attitude Control System (CEACS)". The power generator is typically an array of solar cells, either attached to the spacecraft exterior, or to articulate solar panels. A power source is required during the eclipse periods and the peak power demands. The power source typically comprises a battery made of electrochemical cells, such as nickel cadmium, nickel hydrogen or lithium ion cells. As with any technology, there are some limitations associated with chemical batteries. The number of charge-discharge cycles is limited, and in general, this is the limiting factor on the satellite lifetime. The flywheels have a higher Depth of Discharge (DoD), a longer life cycle and the temperature independence. The concept for using flywheels is to convert an electrical energy to a rotational (kinetic) energy for storage using a motor to spin up the flywheel. Then, the flywheel runs a generator to convert the mechanical energy to an electrical energy when the electrical energy is needed. Accepting a higher charge/discharge rate, a flywheel energy storage system can be simpler and less massive than a battery system.

In space application the rotating flywheels can also perform the attitude control for spacecraft. By integrating the energy storage and attitude control functions, significant mass savings is possible [1]. The CEACS consists of a composite flywheel, magnetic bearings, a motor/generator and control elements for the energy and attitude management [1-5]. A higher rotational speed is expected in order to achieve a higher energy storage capability [6, 7]. In the past years, this application was limited for large satellites [5]. In the case of small satellites, the magnetic bearing causes magnetic interference to the iron parts of the motor-

generator [8]. Therefore, the use of ironless motor-generator for this combined system is essential, which will ensure the CEACS flywheels to be controlled efficiently in a torque mode. In the present article each flywheel is controlled strictly in the torque mode. In contrast, the speed mode controlled flywheel has been deeply investigated [3, 4].

This present study is performed as follows: First, a satellite reference mission is chosen to demonstrate the CEACS investigation. Then, the system block diagram is developed with the required transfer functions along with the necessary mathematical models. The models are simulated through Matlab™ for studying the performance in the ideal and non-ideal test cases. Finally, the CEACS performance is discussed from the attitude performance point of view. It is important to mention that the satellite attitude performance of the torque mode is of paramount importance herein. The CEACS energy storage performances are given in the references [3, 4].

The Mission and Strategies: The earth satellite mission is chosen to investigate the satellite attitude performance. The flywheel assembly (2 flywheels) is mounted on the pitch axis. Therefore, the active attitude controlled is engaged on the pitch axis. The bias momentum stabilization is used for this satellite, thus, the stiffness of the roll/yaw plane is required. The detailed constraints for this mission are given in the Table 1 [3].

The initial flywheel speed is set to 1000 rpm, and the expected maximum flywheel speed is about 45000 rpm for the mission [3, 4]. The total peak power requirement of the satellite is 7 W, and the two counter rotating flywheels are operated simultaneously, the power to be supplied by each flywheel is 3.5 W [4]. Spinning-up or spinning-down the counter rotating flywheels will occur constantly due to the energy requirement. The attitude

Table 1: Mission Constraints

Constraints	Description
Mission duration	2 years
Orbit	Circular at 500 km with inclination of 53°
Eclipse period T_{eclipse}	36.4 min
Mass	10 kg for a size of $0.22 \times 0.22 \times 0.22 \text{ m}^3$
Peak Power	7 W
CEACS mass allocation	2 kg (flywheel allocation $0.18 \text{ kg} \times 2$)
Attitude accuracy (Local Vertical/Local Horizontal coordinate frame (LVLH))	Roll (X) and Pitch (Y) $< 0.2^\circ$, Yaw (Z) $= 0.5^\circ$
Initial pitch bias angular momentum	1.25 N ms
Flywheel inertia I_w	$1.3 \times 10^{-3} \text{ kg m}^2$
Pitch external disturbance torque $T_{D,Y}$	$3.8 \times 10^{-3} + 3.8 \times 10^{-3} \sin(\Omega_0 t) \text{ Nm}$
Eclipse energy supply capacity	4.2 W h

command will always brake one flywheel and spin-up its counter rotating member. The speed pattern of the two counter rotating flywheels will be in such a manner so that the flywheel speeds will converge to neutralize the external disturbance torques. As a result, the system's bias momentum will decrease with respect to the orbital period.

The CEACS Architecture

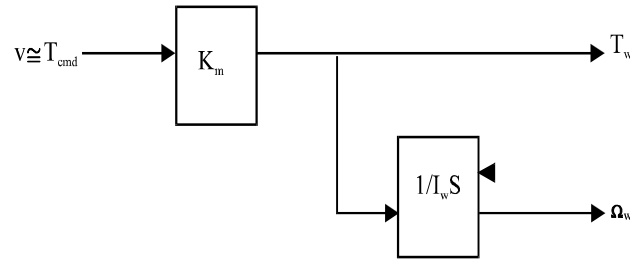


Fig. 1: A Flywheel is Controlled in a Torque Mode

Figure 1 shows a torque controlled flywheel where the relevant transfer functions for the induced flywheel torque T_w and the resulting speed Ω_w are

$$\frac{T_w}{T_{cmd}} = K_m \tag{1}$$

$$\frac{\Omega_w}{T_{cmd}} = \frac{K_m}{I_w s} \tag{2}$$

Here, s denotes the Laplace variable and the motor/generator torque constant K_m is assumed as unity [4]. In this torque control mode the magnetic bearings provide a friction free motion. The attitude control design is shown in Fig. 2. The satellite motion is influenced by the flywheel torque; and therefore, an identical counter rotating partner must be employed to compensate for the torque produced during the charging and discharging phases [1-5].

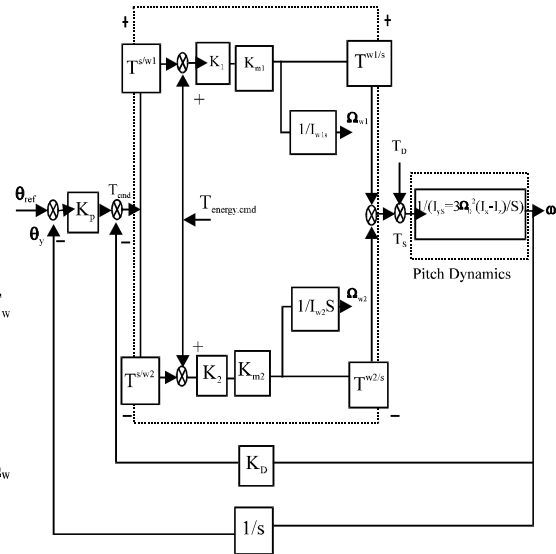


Fig. 2: A Torque Mode CEACS Attitude Control Architecture

Each flywheel is controlled in the torque mode as mentioned earlier. The attitude control command T_{cmd} is issued by the Proportional-Derivative (PD) controller. The attitude control system is designed with a double feedback attitude input, the angle θ_y and angular rate ω_y . These may be produced from star sensor or a gyroscope, respectively. It can be noted that $T^{s/w1}$ is a projection matrix from the satellite coordinate frame to the first flywheel coordinate frame and $T^{w1/s}$ is a projection matrix from the first flywheel coordinate frame to the satellite coordinate frame. Both have a scalar value of 1. On the other hand, $T^{s/w2}$ and $T^{w2/s}$ are the projection matrices for the second flywheel and have a scalar value of -1. It is assumed that the roll (I_x) and yaw (I_z) inertias are similar. Additionally, the inertias for both flywheels and other constants are considered to be equal, i.e.,

$$I_x = I_z,$$

$$I_{w1} = I_{w2} = I_w,$$

and

$$K_1 = K_2 = K.$$

Let $2KK_m = 1$; hence, the associated transfer function for the pitch dynamics is:

$$\frac{\theta_y}{\theta_{ref.}} = \frac{1}{1 + \frac{K_D}{K_P} s + \frac{I_y}{K_P} s^2} \quad (3)$$

or

$$\frac{\theta_y}{\theta_{ref.}} = \frac{1}{1 + 2\zeta \frac{s}{\omega_n} + \frac{s^2}{\omega_n^2}} \quad (4)$$

To eliminate any overshoot of the attitude command, the active control loop damping ratio $\zeta = 1$ is chosen. When the disturbance torque is taken into consideration, then, the transfer function is:

$$\frac{\theta_y}{T_D} = \frac{1}{I_y s^2 + K_{DS} + K_P} \quad (5)$$

The corresponding natural frequency for the close loop system is determined. The proportional control gain K_P and the derivative control gain K_D can be computed as well. The attitude error at the steady state condition can be estimated from the Eq. (5). The flywheels are counter rotating such that the net torque generated during the charging/discharging operations will be nullified.

The CEACS Performance: The calculated parameters are: the proportional control gain $K_P = 0.002177$ Nm/rad, the natural frequency $\omega_n = 0.1639$ rad/s and the damping ratio $\zeta = 1$. The estimated derivative attitude control gain is $K_D = 0.02656$ Nm s/rad. The closed loop poles are found in the left side of the imaginary axis. In this regards, the system is stable. Depending on the internal and external disturbances the CEACS models are investigated through numerical treatments for different ideal and non-ideal test cases incorporating all the preceding parameters.

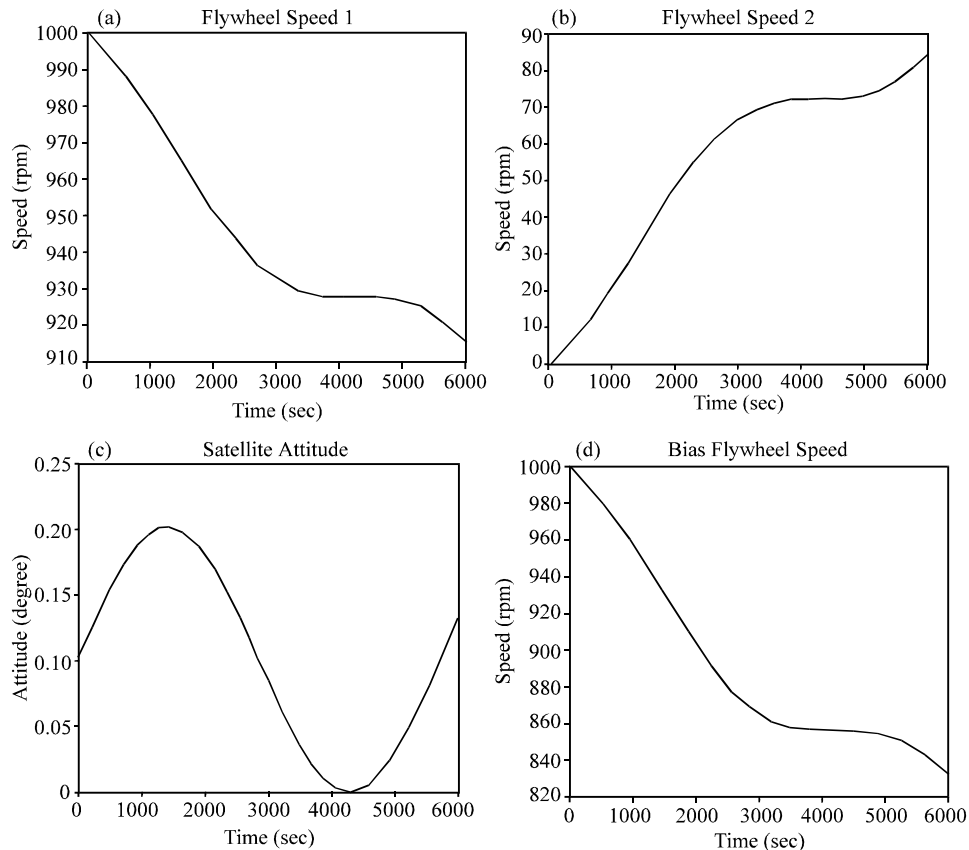


Fig. 3: An Ideal CEACS Performance for an Orbit

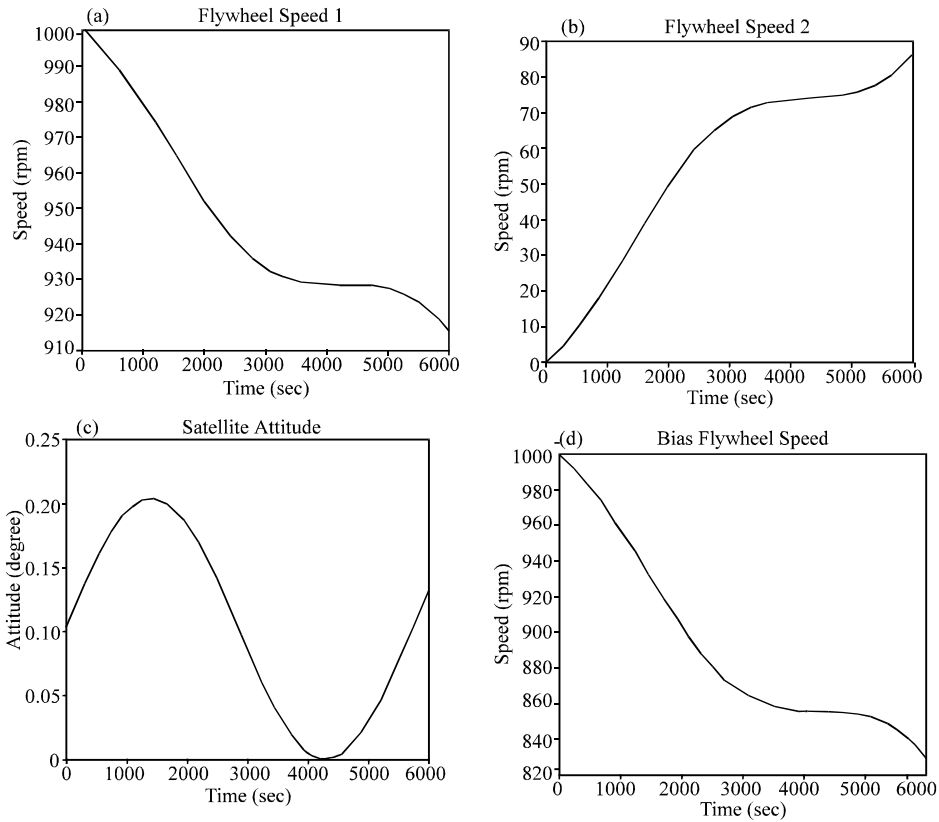


Fig. 4: A Non-ideal CEACS Performance for the Test Case (A)

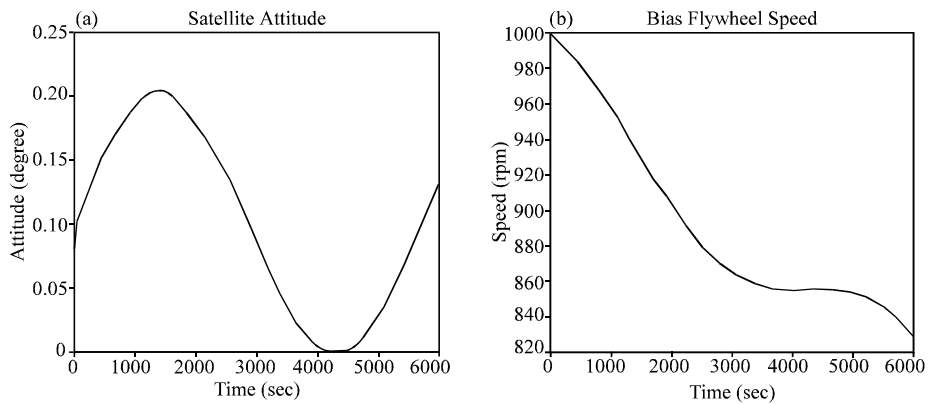


Fig. 5: A Non-ideal CEACS Performance for the Test Case (B)

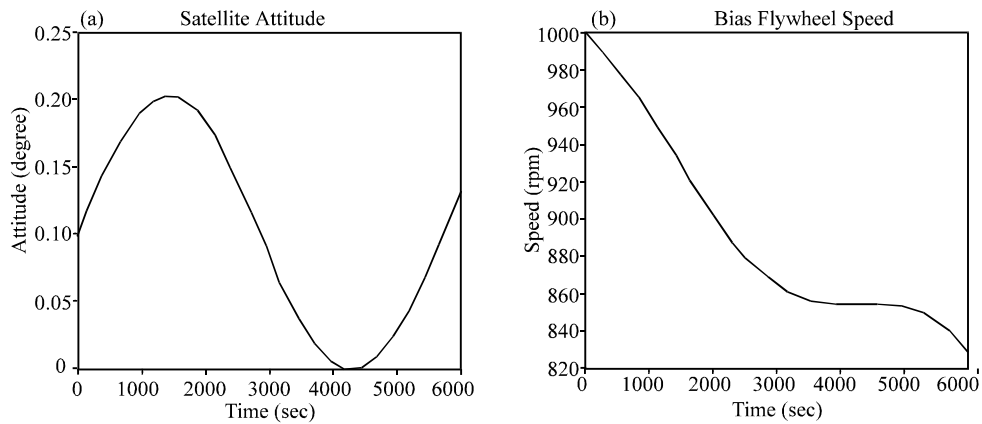


Fig. 6: A Non-ideal CEACS Performance for the Test Case (C)

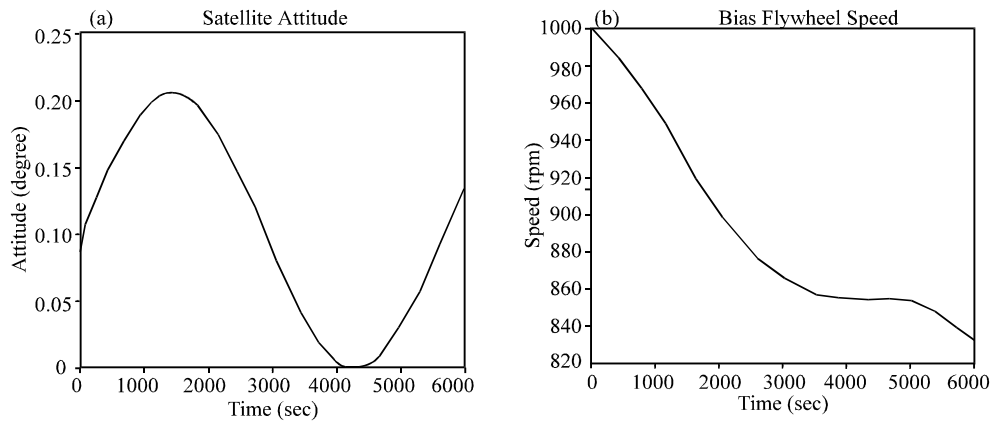


Fig 7: A Non-ideal CEACS Performance for the Test Case (D)

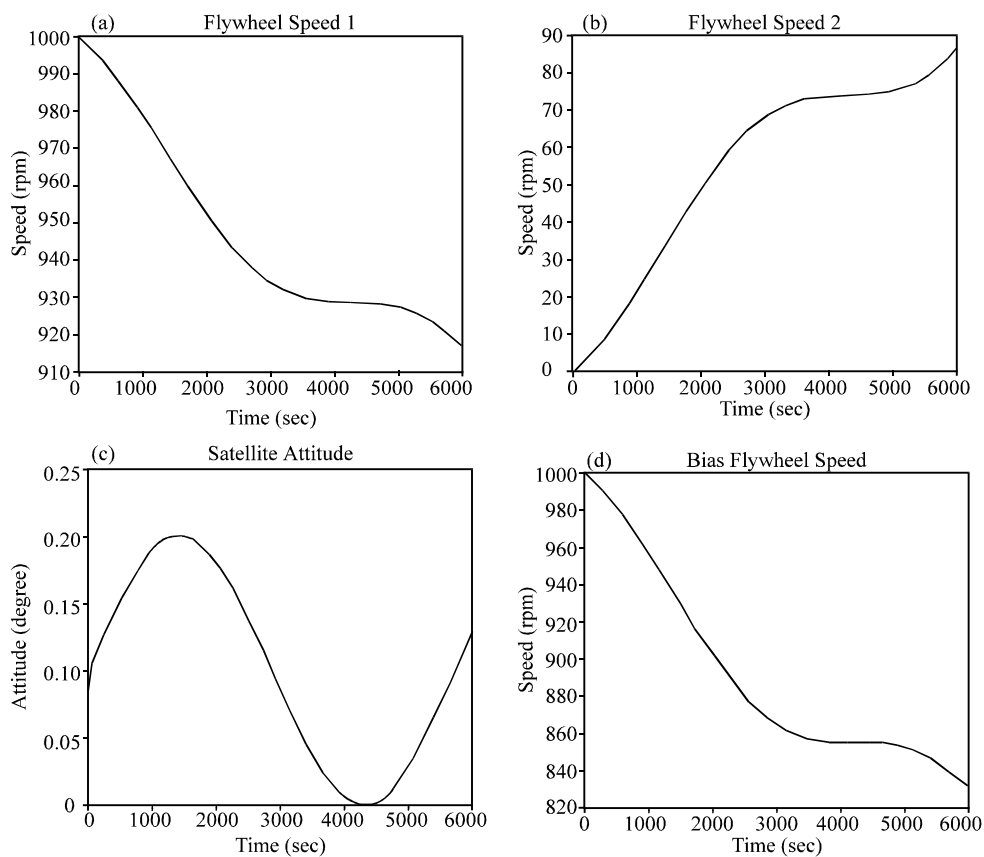


Fig. 8: A Non-ideal CEACS Performance for the Test Case (D). Improved Attitude Performance

Numerical Treatment for an Ideal CEACS: To investigate the performance of an ideal CEACS whereby only the external disturbance torques acting on the satellite are considered. The motor/generator constants are taken as unity and the inertias of both flywheels are at their nominal values. The speeds for 1st and 2nd flywheels are shown in Figs. 3a and b. In this numerical simulation the speed of the 1st flywheel was set to 1000 rpm initially. Figure 3c shows that the attitude error remains within the pointing budget. Bias flywheel speed is shown in Fig. 3d; it generates the required bias angular momentum along the pitch axis to

provide stiffness for the roll/yaw plane. This ideal simulation validates the developed CEACS architecture.

Numerical Treatment for Non-ideal CEACS: The non-ideal CEACS numerical treatment is performed with the internal disturbances and the external disturbance torques acting on the satellite. The relative differences between the motor/generator torque constants and the flywheels' inertias produce the internal gain errors. Therefore, the system was tested for the relative difference of 2% in the motor/generator

constants and for the 1% relative difference in the flywheel inertias. Four test cases are evaluated:

(A) $-K_{m1}, +I_{w1}, K_{m2}, -I_{w2}$; (B) $K_{m1}, -I_{w1}, -K_{m2}, +I_{w2}$; (C) $K_{m1}, +I_{w1}, -K_{m2}, -I_{w2}$; and (D) $-K_{m1}, +I_{w1}, -K_{m2}, -I_{w2}$. The sign +/- indicates whether the constant or inertia is above or below the nominal value. The speed and attitude performances for the test case (A) are presented in Fig. 4. Here the motor/generator constant for the 2nd flywheel system is considered unchanged, and for the 1st flywheel system, the value is reduced 2% from the nominal value. The inertias are taken 1% above and below the nominal value for the 1st and 2nd flywheel, respectively. Due to these relative differences, the attitude accuracy slightly exceeds its budget (Fig. 4c). In the test case (B), the motor/generator constant for the 1st flywheel system is considered unchanged and the value for the 2nd flywheel system is reduced 2% from the nominal value. The inertias are taken 1% below and above the nominal value for the 1st and 2nd flywheels, respectively. Due to the relative differences in the internal gains and inertias, the pitch attitude exceeds its pointing budget in the same manner as in the test case (A) (Fig. 5a).

In the test case (C) the relative differences of motor/generator constants are taken identical as in the test case (B), and the values of inertias are considered the same as in the test case (A). The result of this test shows the similar attitude error magnitude as in the test cases (A) and (B) (Fig. 6a).

The test case (D) investigates the variation of the motor/generator constants of both flywheels with a reduction of 2% from the nominal value. The inertias are identical to the values taken for the test case (A). The attitude accuracy exceeds more drastically the pointing budget, but the bias flywheel speed remains similar (Figs. 7a and b). On the other hand, if the value of the control stiffness K_p is increased by 2% in the test case (D), then, the satellite pitch angle/attitude accuracy respects the pointing budget as shown in Fig. 8c. Hence, the attitude performance for other non-ideal test cases can be improved as well.

In these analyses, Figs. 4-8 represent the CEACS attitude and speed performances for different test cases. The worst case occurs in the test configuration D. In this regards, Fig. 7a shows the impact of these gain errors on the satellite attitude. However, the flywheel speeds (Figs. 4 and 8) and the system bias momentum (Figs. 4-8) are not affected even with these errors; see all figures accordingly. For the test case D, the control stiffness K_p is increased by a factor of 2%, and therefore, the pointing error is improved as shown in Fig. 8c.

CONCLUSION

The CEACS torque mode attitude analysis has been successfully performed in this work. Here, it is found that the main source of internal disturbance torque is the gain errors such as the motor/generator constants and the flywheel inertias. It is proven that the relative differences of motor/generator constants and flywheel inertias influence the satellite attitude performance. However, the pointing accuracy can be improved by tightening the proportional attitude control gain. Despite these gain errors, the bias flywheel speed can be still maintained as requested by the defined mission.

REFERENCES

1. Guyot, P., H. Barde and G. Griseri, 1999. Flywheel power and attitude control system (FPACS). 4th ESA Conference on Spacecraft Guidance, Navigation and Control System, ESA-ESTEC, Noordwijk, pp: 371-378.
2. Barde, H., 2001. Energy storage wheel feasibility study. 4th Tribology Forum and Advances in Space Mechanisms, ESA-ESTEC, Noordwijk, pp: 1-26.
3. Varatharajoo, R., 2004. A combined attitude and energy control for small satellites. Acta Astronautica, 54: 701-712.
4. Varatharajoo, R. and S. Fasoulas, 2000. Methodology for the development of combined energy and attitude control systems for satellites. J. Aerospace Sci. Technol., 6: 303-311.
5. Roithmayr, C.M., 1999. International space station attitude control and energy storage experiment: effects of flywheel torque. NASA Technical Memorandum 209100.
6. Gautheir, M., J.P. Roland, H. Vaillant and A.A. Robinson, 1987. An advanced low-cost 2 axis active magnetic bearing flywheel. 3rd European Space Mechanism and Tribology Symposium (ESMATS), Madrid, pp: 177-182.
7. Kirk, J.A., J.R. Schmidt, G.E. Sullivan and L.P. Hromada, 1997. An open core rotator design methodology. Aerospace and Electronics Conference, NAECON, Dayton, pp: 594-601.
8. Scharfe, M., T. Roschke, E. Bindl and D. Blonski, 2001. Design and development of a compact magnetic bearing momentum wheel for micro and small satellites. 15th AIAA/USU Conference on Small Satellites, Logan, Utah, pp: 1-9.